

---

Aug 24th, 12:00 AM - Aug 25th, 12:00 AM

## Numerical and Experimental Investigation of Cold-formed Steel Double Angle Members under Compression

W. F. Maia

L. C. M. Vieira Jr.

B. W. Schafer

M. Malite

Follow this and additional works at: <https://scholarsmine.mst.edu/isccss>



Part of the [Structural Engineering Commons](#)

---

### Recommended Citation

Maia, W. F.; Vieira, L. C. M. Jr.; Schafer, B. W.; and Malite, M., "Numerical and Experimental Investigation of Cold-formed Steel Double Angle Members under Compression" (2012). *International Specialty Conference on Cold-Formed Steel Structures*. 1.

<https://scholarsmine.mst.edu/isccss/21iccfss/21iccfss-session2/1>

This Article - Conference proceedings is brought to you for free and open access by Scholars' Mine. It has been accepted for inclusion in International Specialty Conference on Cold-Formed Steel Structures by an authorized administrator of Scholars' Mine. This work is protected by U. S. Copyright Law. Unauthorized use including reproduction for redistribution requires the permission of the copyright holder. For more information, please contact [scholarsmine@mst.edu](mailto:scholarsmine@mst.edu).

## NUMERICAL AND EXPERIMENTAL INVESTIGATION OF COLD-FORMED STEEL DOUBLE ANGLE MEMBERS UNDER COMPRESSION

W. F. Maia<sup>1</sup>, L. C. M. Vieira Jr.<sup>2</sup>, B. W. Schafer<sup>3</sup>, and M. Malite<sup>4</sup>

### Abstract

This paper presents a numerical and experimental study of double angle members connected by batten plates under concentric and eccentric axial compression. The number of batten plates is varied to study the influence on the nominal axial strength. Numerical analyses are able to accurately predict the behavior and strength found in the experiments, except for long columns under eccentric axial compression where the composite section failed in major-axis flexural buckling. Two design hypotheses are compared to the results obtained: (i) non-composite action (no interaction between angles), with only local, flexural, and flexural-torsional buckling considered; (ii) composite action (full interaction between angles), and only considering local and minor-axis flexural buckling of the pair of angles. The two design hypotheses ignore load eccentricity. Numerical and experimental results for angles connected by bolted batten plates fall in between the design curves defined by methods (i) and (ii), while angles connected by welded batten plates have greater strength than the design curve defined by method (ii). The use of batten plates significantly increases the strength of the system, especially for members under eccentric compression. However, the strength remains constant after a certain number of batten plates are connected, and after a minimum batten plate width is reached.

---

<sup>1</sup> Ph.D. candidate, Department of Structural Engineering, School of Engineering of Sao Carlos, University of Sao Paulo, Sao Carlos, SP, Brazil

<sup>2</sup> Assistant Professor, Department of Mechanical, Civil and Environmental Engineering, University of New Haven, West Haven, CT, USA

<sup>3</sup> Professor, Department of Civil Engineering, Johns Hopkins University, Baltimore, MD, USA

<sup>4</sup> Professor, Department of Structural Engineering, School of Engineering of Sao Carlos, University of Sao Paulo, Sao Carlos, SP, Brazil

## Introduction

Double-angle members with batten plates consist of two identical angles set up in parallel, spaced apart, and connected to each other by batten plates at specified points along the length. The system presented herein is widely used, especially in light truss structures; however, there are no standard design procedures specific for the design of this structural component.

Traditional hot-rolled steel angles, due to their compact legs, are less prone to local buckling and flexural-torsional buckling for typical lengths. However, cold-formed steel angles, which typically have thin walls (high width/thickness ratios) are subjected to two buckling modes: (i) a global flexural mode, that is dominant for long members, and (ii) a coincident local-plate/global flexural-torsional mode, which is critical for shorter members. It is worth mentioning that simple angles have no primary warping, therefore the warping constant is approximately zero, and as a result flexural-torsional buckling does not depend on the length of the member.

This paper investigates the interaction between buckling modes and the partial composite behavior of double angles connected by batten plates. A finite element (FE) model generated in ANSYS (2011) is used for better understanding the elastic and collapse behavior of simple and lipped double angle members connected by batten plates. Laboratory tests are compared to the FE models.

### 1. Experimental analysis

A series of laboratory tests were conducted on cold-formed steel double angles (2L 60x2.0), cold-formed steel lipped double angles (2Le 50x13x2.0), and hot-rolled steel double angles (2L 50x5.0). The load was either applied to a thick plate (12.5mm) welded to the extremities of the members (concentric load), or to the web of a channel section, which is connected through its flange to one of the legs of the angle (eccentric load), as shown in Figure 1.

The end conditions of the cold-formed steel lipped double angle members (2Le 50x13x2.0) and hot-rolled steel double angle members (2L 50x5.0) were designed as fixed. The end conditions of the cold-formed steel simple double angle members (2L 60x2.0) were fixed about the major axis of the pair of angles and fixed in warping, but designed to allow free rotation about the minor axis of the pair of angles. In this last case, the buckling length ( $L_c$ ) is assumed to be  $L_{\text{member}} + 135$  mm, i.e., corresponding to the distance between the upper and lower support devices of the testing machine (knife-edge device).

Members with different slenderness and different numbers of batten plates were tested. Bolted batten plates were typically used throughout in the tests. Since the batten plates were not damaged during the tests, they were reused in subsequent testing. To understand the difference between welded and bolted batten plates, in one case, the lipped double angle member (2Le 50x13x2.0), testing was conducted with both welded and bolted batten plates.

Since hot-rolled steel double angle members (2L 50x5.0) are not prone to local and flexural-torsional buckling, they serve as a compact cross-section reference to cross-sections with high width/thickness ratios (cold-formed steel angles). The hot-rolled double angles were tested under concentric and eccentric axial load for only one length, but with differing numbers of batten plates. The mechanical properties of the steel for each cross-section are provided in Table 1.

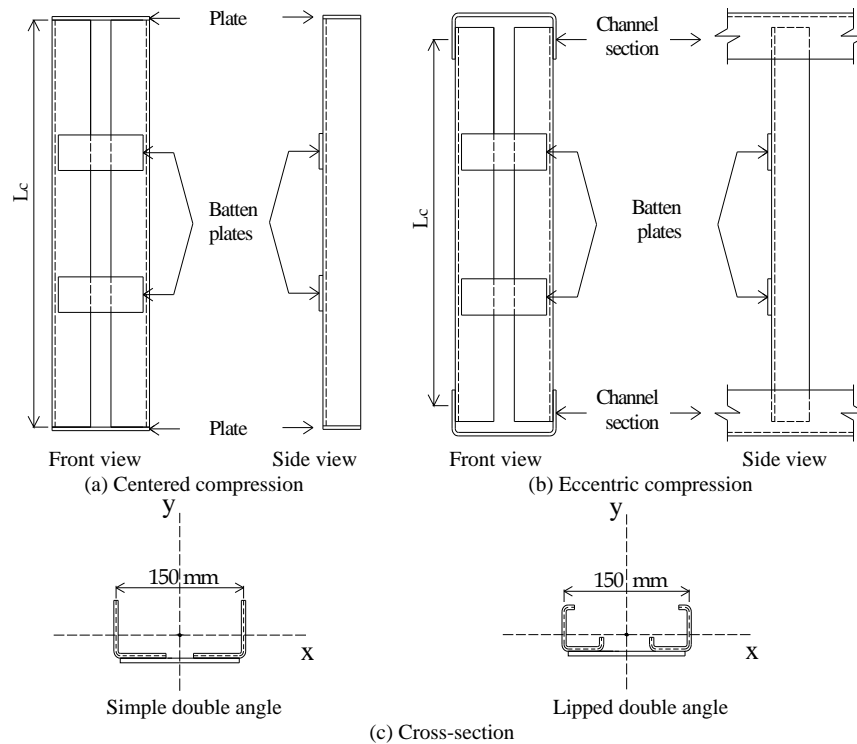


**Figure 1 – Summary of typical arrangements for numerical and experimental tests of simple and lipped double angles**

**Table 1 – Summary of cross-section sizes and mechanical properties of steel.**

Section	Leg (mm)	Lip (mm)	Thickness (mm)	$F_y$ (MPa)	$f_u$ (MPa)	$E^{(1)}$ (MPa)
L 60x2.00	60.0	-	2.00	350	499	200,000
L 50x5.00	50.8	-	4.76	307	455	200,000
Le 50x13x2.00	50.0	13.0	2.00	350	499	200,000

$F_y$  – Yield stress of steel;  $f_u$  – Tensile strength;  $E$  – Modulus of elasticity of steel;  
<sup>(1)</sup> Conventional value

## 2. Numerical analysis

A finite element numerical analysis was performed using ANSYS (2011). The element SHELL 181 was used to model the angles and the channel sections connected at the extremities of the pairs of angles in the eccentric axial load case. According to the ANSYS manual (2011), element SHELL 181 is ideal for non-linear analysis of thin elements subjected to large strains and rotations. The knife-edge device responsible for allowing free rotation in the minor axis was modeled using the element SOLID 45.

The strategy used for applying an initial imperfection to the FE model was the same as used by Maia et al. (2010). Based on an eigenvalue analysis, the critical modes of interest were visually selected for each member: coincident local/flexural-torsional and flexural for the double angle members; local, flexural-torsional and flexural for the lipped double angle members. The new geometry consists of scaling the selected eigenvector according to the initial imperfection values (type 1 and 2) recommended in Schafer & Peköz (1998).

For the double angle members, the coincident local/flexural-torsional buckling mode was scaled to the type 2 imperfection. For the lipped double angle members, the local buckling mode was scaled to the type 1 imperfection, and the flexural-torsional buckling mode was scaled to the type 2 imperfection. An initial imperfection of  $L_c/1500$  was applied to the flexural buckling mode of both cross-sections.

Two approaches were used to model the batten plates: (i) all displacements of two neighbor nodes are coupled where the batten plate is attached, and (ii) the batten plates were modeled, and the displacements were coupled at the connection between batten plate and the angle leg.

### 3. Results

Two design hypotheses, based upon recommendations in ANSI/AISI S100:2007, for axial compressive strength were compared to test results. The first hypothesis considered every angle as a single member independent of the batten plates (non-composite action), and thus explores local, flexural-torsional and flexural buckling of each member individually. The second hypothesis considered only local and flexural buckling (minor-axis) of the composite section.

#### 3.1. Double angle

Table 2 compares the experimental analysis results of the cold-formed steel double angle (2L 60x2.0) to the numerical analysis results and the design hypotheses. Double angle members were tested only with bolted batten plates. The experimental results are compared to the numerical simulation values in which the nodes are coupled but the batten plate is not modeled. The geometry of the FE models was scaled to an initial imperfection of  $0.64t$  for the coincident local/torsional-flexural mode and  $L_c/1500$  for the flexural buckling mode. Figure 2 shows the experimental analysis results compared to the design hypotheses (composite and non-composite action). Figure 3 shows the typical buckling modes observed in the numerical and experimental analyzes.

**Table 2 – Theoretical and experimental analysis results: section 2L 60x2.0**

Member	$P_{test}$ (kN)	Failure mode	$P_{FE}$ (kN)	Failure mode	$P_{test}/P_{FE}$
Fixed ends (eccentric compression)					
L 600-0	72.2	FT/F*	71.6	FT/F*	1.01
L 600-1	74.0	FT	69.2	FT/F	1.07
L 600-2	76.0	FT	75.1	FT/F	1.01
$P_n^{(1)} = 30.5$ kN	$P_n^{(2)} = 76.8$ kN				
L 1200-0	58.5	FT/F*	48.8	FT/F*	1.20
L 1200-0	50.4	FT/F*	48.8	FT/F*	1.03
L 1200-1	55.4	FT/F	52.6	FT/F	1.05
L 1200-2	50.6	FT/F	59.5	FT/F	0.85
L 1200-3	56.2	FT/F	67.0	FT/F	0.84

See next page...

... continuation of Table 2

Member	$P_{test}$ (kN)	Failure mode	$P_{FE}$ (kN)	Failure mode	$P_{test}/P_{FE}$
Fixed ends (eccentric compression)					
L 1200-4	62.5	FT/F	70.9	FT/F	0.88
L 1200-5	72.9	FT/F	69.8	FT/F	1.04
$P_n^{(1)} = 29.8$ kN	$P_n^{(2)} = 67.2$ kN				
L 1800-0	34.1	FT/F*	33.4	FT/F	1.02
L 1800-1	45.0	FT/F*	41.6	FT/F	1.08
L 1800-2	42.8	FT/F*	47.0	FT/F	0.91
L 1800-3	41.1	FT/F*	56.8	FT/F	0.72
L 1800-4	53.5	FT/F/F*	60.9	FT/F	0.88
$P_n^{(1)} = 28.7$ kN	$P_n^{(2)} = 53.6$ kN				
L 2400-0	28.8	FT/F*	24.4	FT/F	1.18
L 2400-1	36.5	FT/F/F*	33.7	FT/F	1.08
L 2400-2	40.4	FT/F/F*	34.9	FT/F	1.16
L 2400-5	34.8	FT/F/F*	51.5	FT/F	0.68
$P_n^{(1)} = 19.9$ kN	$P_n^{(2)} = 38.9$ kN				
Fixed ends (concentric compression)					
LC 1200-0	58.0	FT	48.8	FT	1.19
LC 1200-1	61.7	FT	74.0	FT	0.83
LC 1200-2	69.6	FT	79.9	FT	0.87
LC 1200-3	68.1	FT	79.3	FT	0.86
LC 1200-4	70.4	FT	83.7	FT	0.84
$P_n^{(1)} = 30.5$ kN	$P_n^{(2)} = 76.8$ kN				
Free rotation in relation to the minor axis of the pair of angles (eccentric compression)					
L 1200-0	35.5	FT/F*	33.1	FT/F*	1.07
L 1200-1	42.5	FT/F	43.8	FT/F	0.97
L 1200-2	39.4	FT/F	42.0	FT/F	0.94
L 1200-3	44.0	FT/F	47.0	FT/F	0.94
L 1200-4	52.8	FT/F	47.5	FT/F	1.11
$P_n^{(1)} = 29.6$ kN	$P_n^{(2)} = 64.4$ kN				

Legend:  
**LC X-N**  
L – simple angle; C – centered compression; X – length of the member in millimeters;  
N – number of batten plates.  
FT – flexural-torsional buckling of the individual angle; F – flexural buckling of the double angle; F\* – flexural buckling of the individual angle.  
 $P_n^{(1)}$  – calculated based on ANSI/AISI S100:2007 assuming single member (non-composite action).  
 $P_n^{(2)}$  – calculated based on ANSI/AISI S100:2007 assuming double member (composite action) (axis x, see Figure 2).  
K = 0.5 for members with fixed ends (centered compression); K = 1.0 for members with fixed ends (eccentric compression).  
 $r_x = 1.91$  cm (radius of gyration for the smallest inertia axis of the pair of angles (axis x, see Figure 2)).

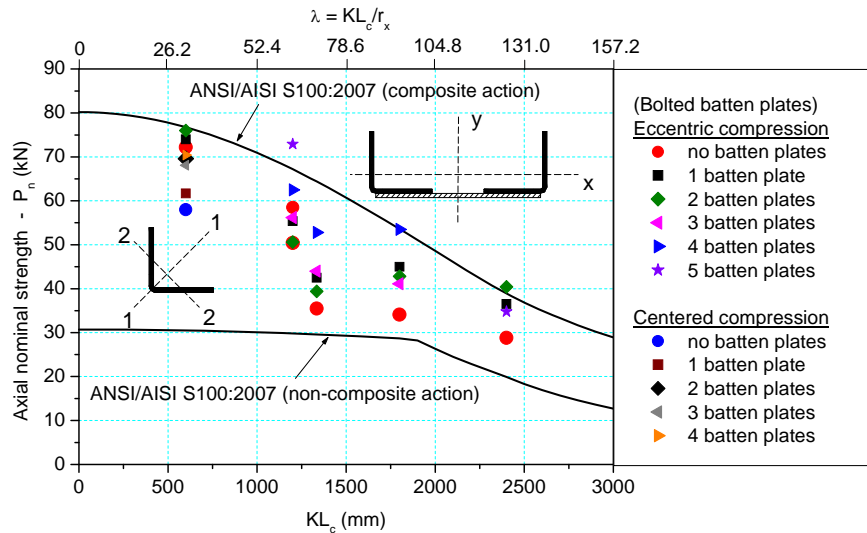


**Figure 2 – Experimental analysis results compared to the design hypotheses (load eccentricity is ignored, section: 2L 60x2.0)**

The predominant buckling mode in the experimental analysis of the cold-formed steel double angle (2L 60x2.0) was flexural-torsional buckling of the single member with half-wave length defined by the spacing between the batten plates. In the case of shorter members, the strength is predominantly defined by flexural-torsional buckling, which does not vary with the member length and therefore the insertion of batten plates does not change the strength of the pair of angles. For longer lengths the insertion of batten plates significantly increased the strength of the member by restraining flexural buckling.

In the numerical analysis, the buckling modes observed were flexural-torsional and flexural in the minor axis of the pair of angles; however, in the experimental analysis it was observed that in addition to these two modes, some members exhibited flexural buckling in the major axis of the pair of angles (parallel to the connected leg). It is possible that the batten plates provide restraint to the rotation parallel to the connected leg, and when flexural buckling occurs in one of the members, the tendency is that the other member follows it. Since the major axis flexural mode was not predicted in the numerical analysis, there is a significant difference in the peak load found in the FE models, compared to the laboratory tests in this case. The simplifications assumed regarding the connection between batten plate and steel angle is a potential source for the difference in the peak load.



By comparing the design hypotheses (composite and non-composite action) to the experimental results, it was observed that for a small number of batten plates the experimental results tend towards the non-composite action hypothesis. An increase in the number of batten plates, however, corresponds to a trend towards the composite action (flexural buckling in the minor axis of the pair of angles).

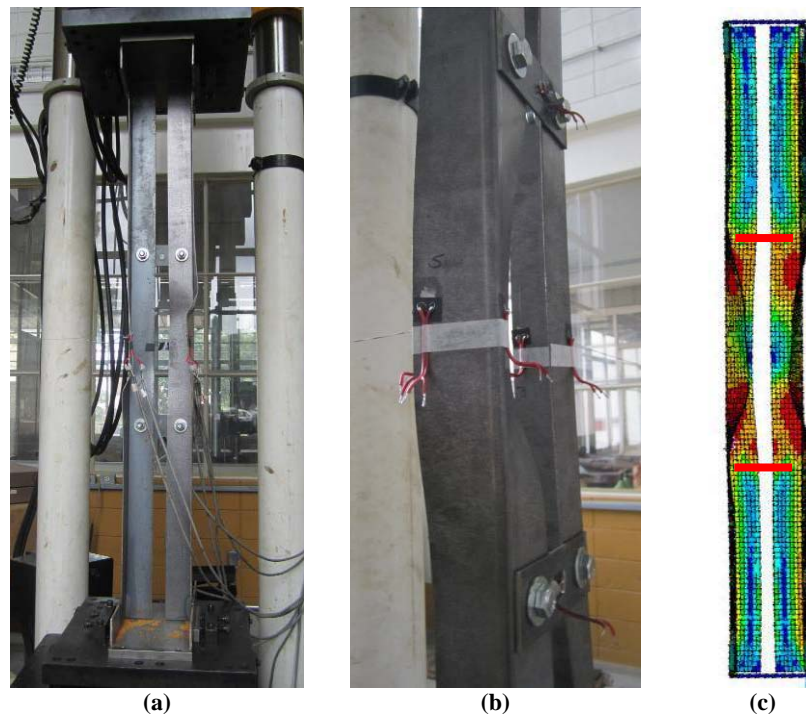


**Figure 3 – Flexural-torsional (FT) and flexural (F) modes – 2 batten plates**  
(a) front view (b) isotropic view, and (c) numerical analysis (eccentric compression)

### 3.2. Lipped-double angle members

Table 3 shows the experimental analysis results of the lipped double angle (2Le 50x13x2.0) compared to the numerical analysis results and the design hypotheses. As mentioned before, lipped-double angle members were tested with bolted and welded batten plates. The experimental results of the members with welded batten plates are compared to the numerical simulation values in which the batten plates were modeled. Similarly, members connected by bolted batten plates are compared to the coupled-node numerical simulation. The

numerical analysis considered initial imperfections of  $0.14t$  for the local mode,  $0.64t$  for the flexural-torsional mode, and  $L_c/1500$  for the flexural mode.

Figure 4 shows the experimental analysis results compared to the design hypotheses. Figure 5 illustrates a typical buckling mode observed in the numerical analysis and experimental analysis.

**Table 3 – Results of theoretical and experimental analysis: section 2Le 50x13x2.0**

Member	$P_{test}$ (kN)	Failure mode	$P_{FE}$ (kN)	Failure mode	$P_{test}/P_{FE}$
Fixed ends (eccentric compression)					
Le 600-0	81.8	FT/F*	80.3	FT/F*	1.02
Le 600-1	111.3	FT	98.3	FT	1.13
Le 600-2	113.6	FT	102.6	FT	1.11
$P_n^{(1)} = 63.7$ kN	$P_n^{(2)} = 149.2$ kN				
Le 1200-0	57.0	FT/F*	54.3	FT/F*	1.05
Le 1200-1	81.1	FT/F/F*	71.5	FT/F	1.13
Le 1200-2	83.4	FT/F*	77.3	FT/F	1.08
Le 1200-3	102.2	FT/F/F*	93.3	FT/F	1.09
Le 1200-4	108.4	FT/F	95.1	FT/F	1.14
$P_n^{(1)} = 38.8$ kN	$P_n^{(2)} = 115.2$ kN				
Le 1800-0	36.4	FT/F*	37.6	FT/F*	0.97
Le 1800-1	62.0	FT/F*	54.3	FT/F	1.14
Le 1800-2	63.2	FT/F/F*	59.3	FT/F	1.07
Le 1800-2(1)	78.3	FT/F	72.8	FT/F	1.08
Le 1800-2(2)	83.4	FT/F	76.1	FT/F	1.10
Le 1800-3	73.9	FT/F/F*	72.8	FT/F	1.02
Le 1800-4	69.3	FT/F/F*	78.3	FT/F	0.89
Le 1800-4(1)	96.2	FT/F	91.6	FT/F	1.05
Le 1800-4(2)	102.4	FT/F	95.2	FT/F	1.08
$P_n^{(1)} = 31.9$ kN	$P_n^{(2)} = 74.9$ kN				
Le 2400-0	18.7	FT/F*	19.9	FT/F*	0.94
Le 2400-1	44.4	FT/F/F*	40.2	FT/F	1.10
Le 2400-2	52.9	FT/F/F*	46.9	FT/F	1.13
Le 2400-5	45.7	FT/F/F*	68.9	F	0.66
$P_n^{(1)} = 20.4$ kN	$P_n^{(2)} = 43.3$ kN				
Fixed ends (centered compression)					
LeC 1200-0	77.1	FT	76.1	FT/F*	1.01
LeC 1200-1	91.3	FT	88.9	FT	1.03

See next page...

... continuation of Table 3

Member	$P_{test}$ (kN)	Failure mode	$P_{FE}$ (kN)	Failure mode	$P_{test}/P_{FE}$
Fixed ends (centered compression)					
LeC 1200-2	108.9	FT	95.6	FT	1.14
LeC 1200-3	115.0	FT	114.0	FT	1.01
LeC 1200-4	107.6	FT	118.6	FT	0.91
$P_n^{(1)} = 63.7$ kN	$P_n^{(2)} = 149.2$ kN				

Legend:

**LC X-N**

Le – lipped angle; C – centered compression; X – length of the member in millimeters; N – number of batten plates.

(M) – welded batten plates – (1): 50 mm wide plate; (2): 100 mm wide plate.

FT – flexural-torsional buckling of the individual angle; F – flexural buckling of the double angle; F\* – flexural buckling of the individual angle.

$P_n^{(1)}$  – calculated based on ANSI/AISI S100:2007 assuming single member (non-composite action).

$P_n^{(2)}$  – calculated based on ANSI/AISI S100:2007 assuming double member (composite action) (axis x, see Figure 4).

$K = 0.5$  for members with fixed ends (centered compression);  $K = 1.0$  for members with fixed ends (eccentric compression).

$r_x = 1.76$  cm (radius of gyration for the smallest inertia axis of the pair of angles (axis x, see Figure 4)).

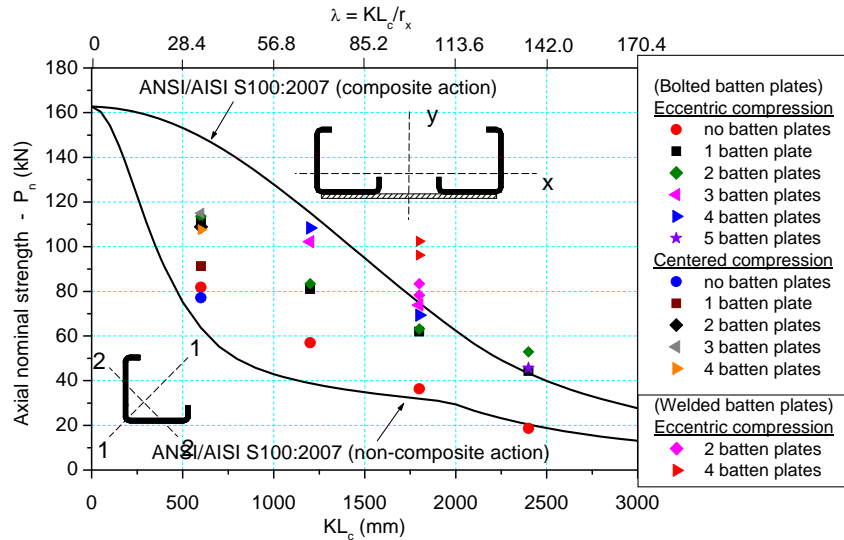
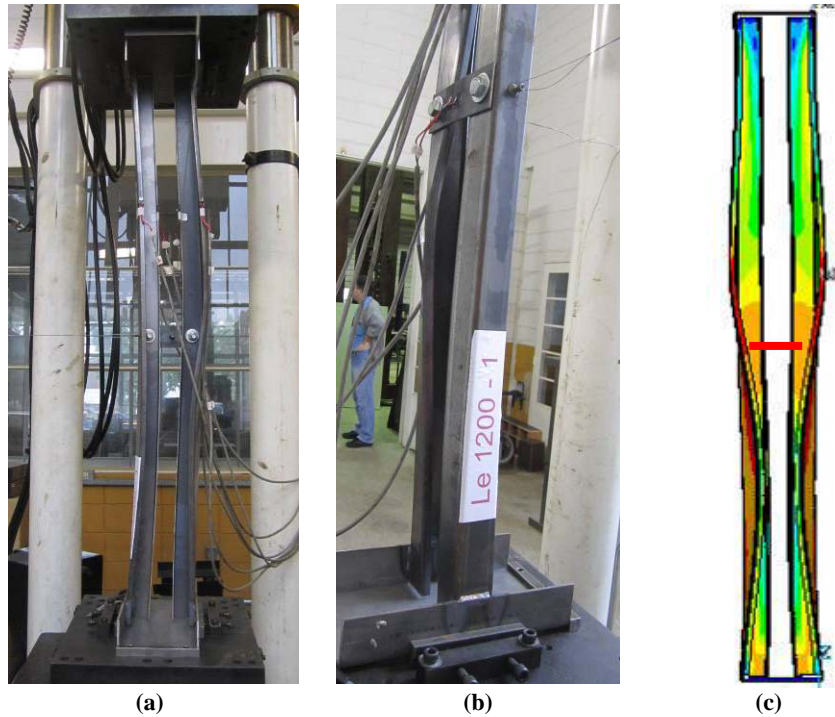


**Figure 4 – Results of the experimental analysis compared to the design hypotheses (load eccentricity is ignored, section: 2Le 50x13x2.0)**



(a) (b) (c)  
**Figure 5 – Flexural-torsional (FT) and flexural (F) modes – 1 batten plate**  
 (a) and (b) experimental and (c) numerical analysis (eccentric compression)

It is worth noting that the warping constant in lipped angles is not negligible, unlike in simple angles: flexural-torsional buckling thus depends on length. For short columns the increase in the number of batten plates significantly increases the strength of the pair of angles. In addition, as noted in the simple angle experiments, a few lipped angle members exhibited flexural buckling about the major axis of the angle pair, a mode not predicted in the numerical simulations.

There was a significant increase in the strength of members with welded batten plates. By doubling their width; however, little change was observed in the results. Strength results of the numerical analysis were consistent with the experimental analysis results.

By comparing the numerical and experimental analysis results to the design hypotheses, the same basic tendencies found for the simple double angles was observed for the lipped double angles. Numerical and experimental results fall in

between the two design hypotheses, but as the number of batten plates increases, the strength approaches the composite action hypothesis.

### 3.3. Hot-rolled steel double-angle members

Table 4 summarizes the experimental analysis, numerical analysis, and the design hypotheses for hot-rolled steel double angles (2L 50x5.0) – only members with bolted batten plates were tested. The numerical simulation results presented herein considered initial imperfections of  $0.14t$  for the flexural-torsional mode and  $L_c/1500$  for the flexural mode. Figure 6 shows the experimental analysis results compared to the design hypotheses.

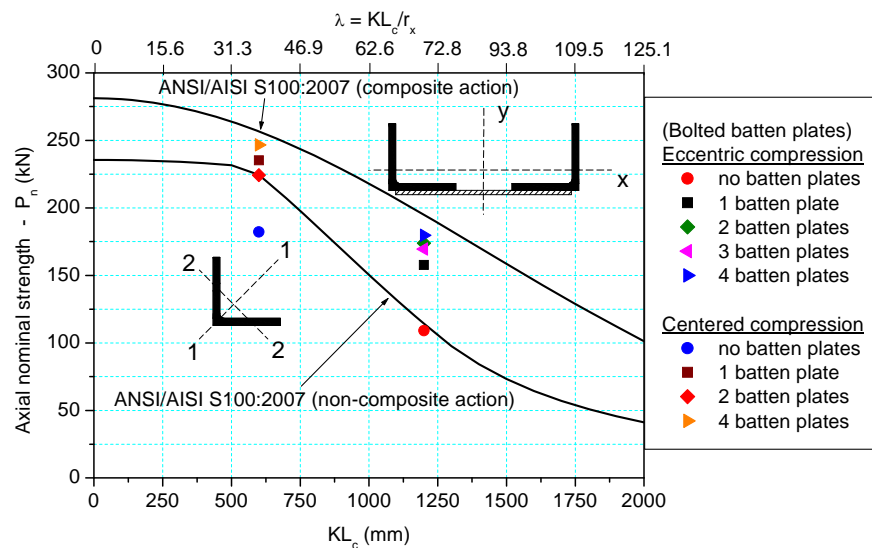


Figure 6 – Experimental analysis results compared to the design hypotheses (load eccentricity is ignored, section: 2L 50x5.0)

**Table 4 – Theoretical and experimental analysis results: section 2L 50x5.0**

Member	$P_{test}$ (kN)	Failure mode	$P_{FE}$ (kN)	Failure mode	$P_{test}/P_{FE}$
Fixed ends (eccentric compression)					
LL 1200-0	109.0	F*	126.0	F*	0.87
LL 1200-1	157.7	F	172.7	F	0.91
LL 1200-2	173.9	F	176.3	F	0.99
LL 1200-3	169.5	F	190.0	F	0.89
LL 1200-4	179.7	F	196.4	F	0.92
$P_n^{(1)} = 114.2$ kN		$P_n^{(2)} = 194.8$ kN			
Fixed ends (centered compression)					
LLC 1200-0	182.1	F*	233.9	F*	0.78
LLC 1200-1	235.2	F	253.1	F	0.93
LLC 1200-2	224.3	F	250.6	F	0.90
LLC 1200-4	246.7	F	253.3	F	0.97
$P_n^{(1)} = 224.5$ kN		$P_n^{(2)} = 256.6$ kN			

Legend:

**LLC X-N**

LL – hot rolled angle; C – centered compression; X – length of the member in millimeters; N – number of batten plates.

F – flexural buckling of the double angle; F\* – flexural buckling of the individual angle.

$P_n^{(1)}$  – calculated based on ANSI/AISI S100:2007 assuming single member (non-composite action);

$P_n^{(2)}$  – calculated based on ANSI/AISI S100:2007 assuming double member (composite action) (axis x, see Figure 6).

$K = 0.5$  for members with fixed ends (centered compression);  $K = 1.0$  for members with fixed ends (eccentric compression).

$r_x = 1.60$  cm (gyration radius for the smallest inertia axis of the pair of angles (axis x, see Figure 6)).

Hot-rolled steel double angles failed in flexural buckling in the major and minor axis of the pair of angles. Once more, experimental results fall in between the two design hypotheses (composite and non-composite action). For hot rolled double angles, however, the strength barely changes due to the increase in the number of batten plates.

#### 4. Conclusions

The experimental and numerical analysis results showed intermediate values to those obtained based on the two design hypotheses, that is, non-composite action (minimum of local, flexural, and flexural-torsional buckling of a single angle), and composite action (local buckling and flexural buckling in the minor axis of the pair of angles). By increasing the number of batten plates, the strength gets closer to the composite action design hypothesis, except for hot-

rolled steel double angles, where the predominant buckling mode is flexural buckling of the pair of angles.

The members connected by welded batten plates, which do not allow rotation of the connection on the plane of the plate, performed better than the corresponding members with bolted batten plates, which allow partial rotation on the plane of the plate. However, by doubling the width of the batten plate, there was little change in the results, demonstrating that the type of connection is more important than the size of the batten plates.

With respect to the numerical analysis, the results were generally consistent with the experimental analysis results, except in cases where the members showed flexural buckling in the major axis of the pair of angles. Research is ongoing to experimentally compare more cases where the strength and behavior of the pair of angles is changed based on the type of connection (welded versus bolted batten plates).

Batten plates significantly increased the strength of double angle members, particularly for members under eccentric compression. However, it was also observed that after a certain number of batten plates are added, the strength tends to remain constant. An interesting observation is that the pairs of angles perform better when there is a batten plate at mid-length. In many cases, members with one batten plate performed better than members with two batten plates.

### **Future Research**

The experimental analysis is still under development concomitantly with the development of a new design method for cold-formed steel double angle members under compression. A final report will be provided at <http://web.set.eesc.usp.br/producao>

### **Acknowledgments**

The authors are grateful to CNPq (National Council for Scientific and Technological Development) for the financial resources granted.

**References**

ANSI/AISI S100:2007. North American specification for the design of cold-formed steel structural members. *American Iron and Steel Institute*. Washington, DC, USA, 2007.

ANSYS. *Structural nonlinearities*. v.13.0, Houston, USA, 2011.

Maia, W. F.; Munaiar Neto, J.; Malite, M.. Theoretical analysis of cold-formed steel battened double angle members under compression. In: LaBoube, R.A.; Yu, W.W. (Ed). *Recent research and developments in cold-formed steel design and construction* (20th International Specialty Conference on Cold-Formed Steel Structures, St. Louis, USA, 2010). University of Missouri-Rolla, 2010.

Schafer, B.W.; Peköz, T. Computational modeling of cold-formed steel: characterizing geometric imperfections and residual stresses. *Journal of Constructional Steel Research*, v.47, 193-210, 1998.